

# Cytotoxic effect of iron nanoparticles *in vitro* on some cell lines

Shatha Salah Asad <sup>1</sup>, Khalid Mahdi Salih <sup>2</sup>, Nahi yousif yassen <sup>3</sup>

<sup>1</sup> Baghdad University ,Al-kindy college of medicine ,Anatomy department/Histology.

<sup>2</sup> Al-Mustansiriya University ,College of science ,Department of biology.

<sup>3</sup>Al-Mustansiriya University, Iraqi Centre for Cancer & Medical Genetics Research.

## Abstract:

**Aim:** Cancer nanotechnology offers great potential for cancer diagnosis, targeted treatment, and monitoring, Among the rapidly evolving types of NPs, magnetic NPs (MgNPs) – biocompatible and superparamagnetic nanomaterials with chemical stability and low toxicity – are especially promising. the biosafety of this material needs to be estimated. the aim of this study evaluate the cytotoxic effect with MgNPs-Fe<sub>3</sub>O<sub>4</sub> on some cancer cell growth *in vitro*. Material and method: Six concentrations of iron oxide nanoparticles (IONP) [(100,200,400,600,800and1000 ) µg/ml] were prepared and tested on Hela, RD and ANM3 cancer cell line in compare with REF cell line as a normal control for( 24 and 48) hr. nine replicates for each concentration ,The optical density of cell growth read by Elisa reader at 500nm, MTT colorimetric assay was employed to estimate the percentage of viable cells after each treatment. Results: All tumor cell lines (RD, HeLa, and AMN3) demonstrated significant reduction in the values of OD and GI% after 24 and 48 hr exposure to all concentrations of iron oxide NPs, while those of Ref cell line revealed non-significant elevation, when correlated with control group .Conclusion: IONP(20-30nm) induced cell cytotoxicity at all concentration when exposed to (Hela ,RD ,and AMN3) cancer cell lines when compared with REF normal cell line.

**Key words:** iron nanoparticles ,*in vitro* , cell lines ,cytotoxicity

## Introduction:

Iron oxide nanoparticles (IONPs) have been used for a variety of biomedical researches and diagnostic purposes, including cancer therapy, cell labeling, drug delivery and magnetic resonance imaging (MRI) [1-4].

Fe<sub>3</sub>O<sub>4</sub>, is very promising, because of its proven biocompatibility [5]. Superparamagnetic iron oxide nanoparticles (SPION), the only clinically approved metal oxide nanoparticles (NPs), hold immense potential in a vast variety of biomedical applications such as magnetic resonance imaging (MRI), targeted delivery of drugs or genes, tissue engineering, targeted destruction of tumor tissue through hyperthermia, magnetic transfections, iron detection, chelation therapy and tissue engineering [5,6,7]. The SPION agents have a unique property of superparamagnetism that confers advantages such as the generation of heat in alternating magnetic fields; or an ability to be guided to a specific tissue or organ by an external magnetic field. They were approved in the EU as a medi-

cal device for magnetic tumor hyperthermia in brain [8] and prostate cancer[9]. Once these nanomaterials are delivered to the tumor site, they efficiently absorb energy from an extrinsic source transforming it into heat due to the reorientation of the magnetization process that disappears as soon as the magnetic field is removed [10]. Unexpectedly, it has been discovered that some nanomaterials have been found to exhibit unexpected enzyme-like activity. For instances, Fe<sub>3</sub>O<sub>4</sub> magnetic nanoparticles (MNPs) actually exhibit an intrinsic peroxidase-like activity, therefore, these nanomaterial-based artificial enzymes are called nanozymes that have already found wide applications in numerous fields, including biosensing, immunoassays, cancer diagnostics and therapy, neuroprotection, stem cell growth, and pollutant removal [11,12]. Due to the nano-size of metal oxide nanoparticles, they can potentially induce cytotoxicity and can manifest themselves by impairing the functions of the major components of the cell, namely mitochondria, nucleus and DNA [13].

### Corresponding Address:

Shatha Salah Asad

Baghdad University, Al-kindy college of medicine, Anatomy department/Histology.

Email: shathasalah95@yahoo.com

## Material and method:

### Cell lines and culture

Four cell lines were obtained from Iraqi Center of Cancer

and Medical Genetics Research, three of them represent tumor cell lines, and the fourth represent normal cell line. The AMN-3 tumor cell line is firstly established by Al-Shammery, (2003)[14] from aged female mouse that had spontaneous mammary adenocarcinoma. The second tumor cell line is RD that is derived from a biopsy specimen obtained from a pelvic rhabdomyosarcoma of a 7 year-old Caucasian girl [Johnston and Siegel, 1990]. The third tumor cell line is HeLa cell line, which is primarily established by Gey et al., (1951)[15] in Johns Hopkins medical school from 31 years old mother named Henrietta Lacks who had cervical carcinoma. However, the last cell line is REF which is transformed rat embryonic fibroblast prepared by Al-Shammery, (2003) [14] and can be used as normal cell line. The cells were cultured in RPMI 1640 medium containing 10% (v/v) fetal calf serum, 100 U/mL penicillin, and 100 µg/mL streptomycin at 37°C in a humidified 5% CO<sub>2</sub> incubator, and passaged once every 2–3 days.

#### Preparation of Iron oxide nanoparticle concentrations

Iron oxide NPs was purchased from Nano Rahpouyan Mahan (NRM)/ Iran, the purity of Fe<sub>3</sub>O<sub>4</sub> NPs is more than 99.5%, dark brown in color with particle size range from 15–20 nm and bulk density about 0.85g/cm<sup>3</sup>. To prepare different concentrations of Fe<sub>3</sub>O<sub>4</sub> nanoparticle, 20 mg of Fe<sub>3</sub>O<sub>4</sub> was initially dissolved in 10 ml of propyl glycol because it is not completely soluble in media, this solution is considered as stock solution with a concentration of 2000 µg/ml. Then from stock solution six concentrations (1000, 800, 600, 400, 200, and 100 µg/ml) were prepared by dilution with serum free media (RPMI free from fetal calf serum).

#### Cell-viability analysis (MTT assay)

The 3-(4,5-dimethylthiazol-2-yl)-2,5-diphenyl-tetrazolium bromide (MTT) colorimetric assay was used to complete cell viability. The MTT assay is based on the ability of a mitochondrial dehydrogenase enzyme from viable cells to cleave the tetrazolium rings of the pale-yellow MTT and form dark-blue formazan crystals that are generally impermeable to cell membranes, thus appear in crystal accumulation in healthy cells. The number of viable cells is directly corresponding to the level of the formazan product formed. The color was quantified using a simple colorimetric assay, with the use of a multiwell scanning spectrophotometer (enzyme-linked immunosorbent assay reader).

For the MTT assays, cells line (~10,000 cells/well) were seeded in 96-well plates, using (~200 µL/well) RPMI medium, and after 24hr seeding, six concentrations of the TiO<sub>2</sub> dispersions were added to the appropriate cell wells and then the cell harvested after 24 and 48 hr. On the day of the viability assay [16], fresh medium removed and 50 µL/well MTT solution (2 mg/mL in phosphate-buffered-saline [PBS]) was added to each well, and the plates were incubated at 37°C for at least 2 hours. At the end of the incubation period, the MTT solution were removed from each well and 130 µL/well dimethyl sulfoxide was added. The 96-well plates were then gently shaken for 15 minutes. In this type of experiment, optical density was measured at 500 nm. The percentage of via-

bility was calculated compared with untreated control (100% viability).

The average of OD for each concentration is determined and used for calculation of the growth index percentage (GI%) according to the following equation [Gao et al., 2003]:

$$GI\% = (B-A/A) \times 100 \dots\dots\dots \text{(Equation 1)}$$

Where GI% is the percentage of growth index, A is the average of optical density of untreated wells, and B is the average of optical density of treated wells. Negative value of GI% means growth inhibition, while positive value means growth improvement.

## Results:

### Effect of Iron oxide NPs

The OD of all tumor cell lines (RD, HeLa, and AMN3) were significantly decreased after 24 hr exposure to different concentrations of iron oxide NPs from those of control groups (0.671 ± 0.082, 1.473 ± 0.132, and 0.836 ± 0.116 respectively) down to (0.172 ± 0.023, 0.303 ± 0.058, and 0.076 ± 0.002 respectively) at concentration of 1000 µg/ml (Table 1). Therefore, their GI% values were significantly reduced until reached to -74.3%, -79.4%, and -90.9% respectively (Figure 1). In contrast, the OD of Ref cell line was significantly increased from 1.305 ± 0.03 in control group up to 1.677 ± 0.164 after 24 hr exposure to 1000 µg/ml concentration of iron oxide NPs (Table 1), and its GI% was significantly improved starting from (32.4%) at concentration of 400 µg/ml reaching to 28.5% at concentration 1000 µg/ml (Figure 1).

**Table 1:** Optical density (OD) of different cell lines after 24 hr exposure to various concentrations of Fe<sub>3</sub>O<sub>4</sub> NPs.

Conc. Of Fe <sub>3</sub> O <sub>4</sub> µg/ml	OD of Cell line (Mean ± SE)			
	RD	HeLa	AMN3	Ref
<b>0 (control)</b>	0.671 ± 0.082	1.473 ± 0.132	0.836 ± 0.116	1.305 ± 0.03
<b>100</b>	0.235± 0.025*	0.459 ± 0.022 *	0.273 ± 0.031*	1.276 ± 0.075
200	0.177 ± 0.022 *	0.495 ± 0.155*	0.156 ± 0.006 *	1.348 ± 0.041
400	0.239 ± 0.029*	0.509 ± 0.100*	0.133 ± 0.020 *	1.728 ± 0.176*
600	0.227 ± 0.016*	0.520 ± 0.073*	0.087 ± 0.004 *	1.676 ± 0.204 *
800	0.171 ± 0.022*	0.505 ± 0.057*	0.091 ± 0.002 *	1.671 ± 0.145*
1000	0.172 ± 0.023*	0.303 ± 0.058*	0.076 ± 0.002 *	1.677± 0.164*

(\*) Significant difference at  $P < 0.05$ , Two-tail by one-way ANOVA test

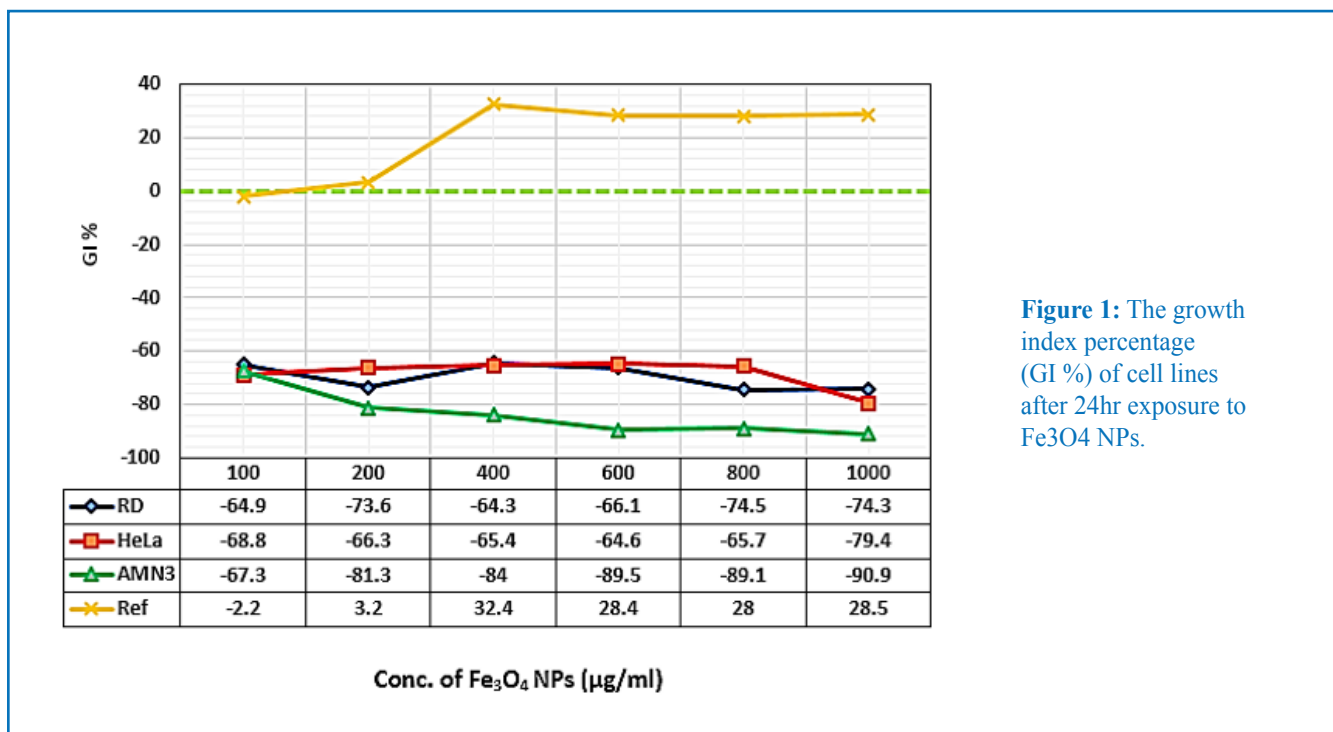


**Figure 1:** The growth index percentage (GI %) of cell lines after 24hr exposure to Fe<sub>3</sub>O<sub>4</sub> NPs.

**Table 2 :** Optical density (OD) of different cell lines after 48 hr exposure to various concentrations of Fe<sub>3</sub>O<sub>4</sub> NPs.

Conc. Of Fe <sub>3</sub> O <sub>4</sub> µg/ml	OD of Cell line (Mean ± SE)			
	RD	HeLa	AMN3	Ref
0 (control)	1.477 ± 0.025	1.410 ± 0.224	0.983 ± 0.059	0.135 ± 0.038
100	0.702 ± 0.048*	0.204 ± 0.031*	0.814 ± 0.017	0.120 ± 0.005
200	0.617 ± 0.127*	0.071 ± 0.005*	0.667 ± 0.020*	0.132 ± 0.006
400	0.558 ± 0.067*	0.072 ± 0.007*	0.664 ± 0.048*	0.150 ± 0.013
600	0.657 ± 0.052*	0.063 ± 0.004*	0.610 ± 0.090*	0.184 ± 0.005
800	0.567 ± 0.044*	0.079 ± 0.007*	0.403 ± 0.102*	0.225 ± 0.024
1000	0.467 ± 0.042*	0.074 ± 0.003*	0.109 ± 0.010*	0.176 ± 0.020

(\*) Significant difference at P < 0.05, Two-tail by one-way ANOVA test

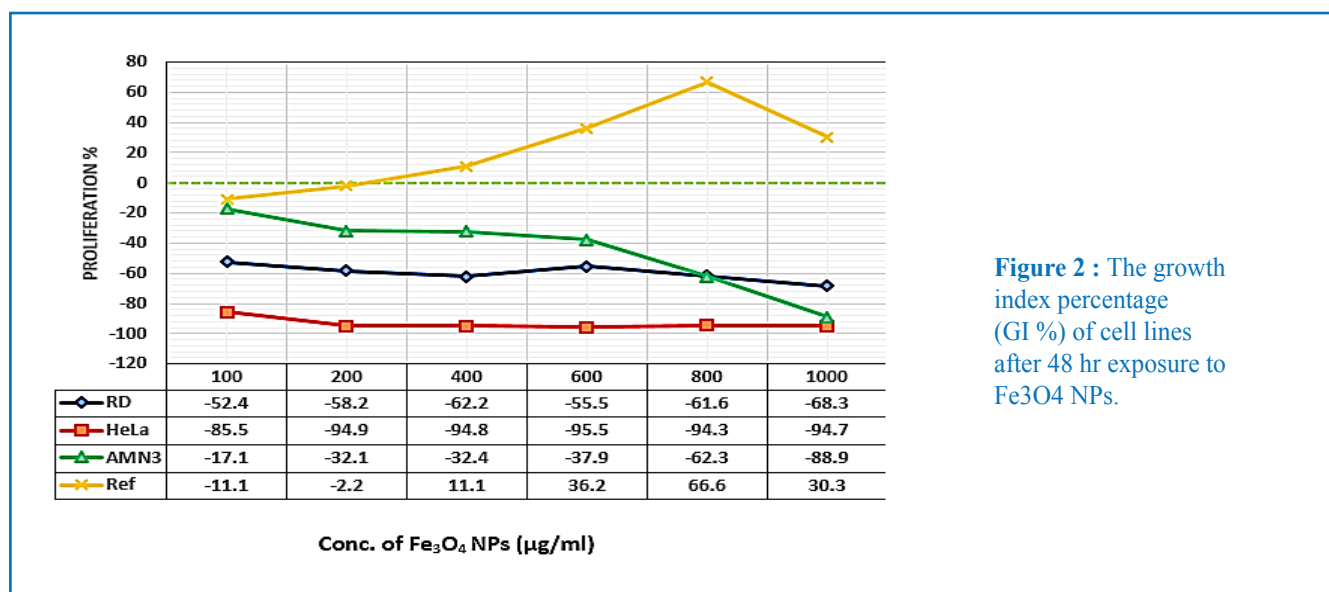


**Figure 2 :** The growth index percentage (GI %) of cell lines after 48 hr exposure to Fe<sub>3</sub>O<sub>4</sub> NPs.

Although all concentration of iron oxide NPs caused significant change in the GI% of all cell lines, there is non-significant correlation between concentration and GI% except in AMN3 cell line that showed significant reverse correlation at

both periods of exposure (24 hr, and 48 hr), and in Ref cell line that revealed significant direct correlation just after 48 hr of exposure (Table 3).

**Table 3 :** Correlation coefficient (R) of Fe<sub>3</sub>O<sub>4</sub> NPs concentration with GI% of different cell lines.

Exposure period		Fe <sub>3</sub> O <sub>4</sub> NPs concentration vs GI % of			
RD		HeLa	AMN3	Ref	
24 hr	R	0.5375 -	0.5213 -	-0.8479	0.7686
	P	0.271	0.288	0.033	0.074
hr 48	R	-0.7746	-0.5553	-0.9418	0.8162
	P	0.070	0.252	0.005	0.047

Negative R value means reverse correlation, Positive R value means direct correlation by Pearson test, Any P value < 0.05 means Significant correlation

## Discussion:

Similarly, all tumor cell lines (RD, HeLa, and AMN3) demonstrated significant reduction in the values of OD (Table 2) and GI% (Figure 2) after 48 hr exposure to all concentrations of iron oxide NPs, while those of Ref cell line revealed non-significant elevation. Discussion

The present study found that 24 hr and 48 hr exposure of different tumor cell lines to various concentration (100–1000 µg/ml) of Fe<sub>3</sub>O<sub>4</sub> NPs caused significant reduction in their growth index by using MTT assay, while that of Ref cell line was significantly improved (Figure 1 & 2). Iron oxide nanoparticles (IONPs) including Fe<sub>2</sub>O<sub>3</sub> and Fe<sub>3</sub>O<sub>4</sub> NPs are one of the most versatile and safe nanoparticles in a wide variety of biomedical applications. In the past decades, considerable efforts have been made to investigate the potential adverse biological effects and safety issues associated with SPIONs [17].

in vitro studies conducted with IONPs shed light on changes in membrane integrity, metabolic activity, and genetic material of cells upon reacting with IONPs. In vitro nanotoxicity assessments can produce reliable and reproducible results which are highly affected by certain parameters such as types of NPs, cells, cell culture conditions, and assay protocols [18,19,20].

In respect to the type of cell line, IONPs have been tested with a variety of cell lines such as human epidermal keratinocytes, human lung epithelial cell lines, BRL3A rat liver cells, and Cos-7 monkey fibroblasts which revealed variations in in vitro toxicity results [21]. Also it has been found that amine-modified IONPs induced 25% reduction in cell viability of astrocytes from a mouse brain derived endothelial cell line at a concentration of 224 µg/mL, whereas the same treatment showed little reduction in human dermal fibroblasts and human fibrosarcoma cells at the same concentration [22]. This variability in responses to iron oxide NPs treatment may be due to different level in expression of transferrin receptor which is a crucial protein involved in iron homeostasis and the regulation of cell growth. The high levels of expression of transferrin receptor in cancer cells, which may be up to 100-fold higher than the regular expression of normal cells, its extracellular accessibility, its ability to internalize and its central role in the cellular pathology of human cancer, make this receptor an attractive target for cancer therapy [23].

On the other hand, dose dependent effects of IONPs have been verified with different cell types. Many studies have demonstrated that at doses of 100 µg/mL or higher, IONPs with varying physicochemical characteristics may cause low toxicity or cytotoxicity due to generation of excessive reactive oxygen species (ROS), which subsequently transferred to the interior of the cell where they can produce oxidative stress by activating transcription factors for pro-inflammatory mediators [24,25]. The entrance of nanoparticles into cells revealed that the majority of nanoparticles existed in cytoplasm in a collective format. The amount of nanoparticles in cells was dependent on the dose and incubating time acting

to cells [26]. Moreover, studies conducted with murine macrophage [27] and human lung alveolar epithelial cells [28] found that the cell death associated with increasing concentration is due to the generation of ROS mediated oxidative stress. Recently, it was found that IONPs often induce cytotoxicity at concentrations greater than 300 µg/mL and prolonged exposure time [29].

The cytotoxicity of IONPs was found to be highly dependent on a range of factors related to their physical properties, such as size, shape and surface coating. These physicochemical parameters of IONPs also contribute towards ROS induction in cells. For example, the shape of IONPs has a varying degree of response towards toxicity as rod shaped IONPs (Fe<sub>2</sub>O<sub>3</sub>) showed a higher degree of necrosis in mouse macrophage cells than spherical IONPs did. Rod-shaped IONPs were mostly accumulated in the cytoplasm, while spherical IONPs aggregated in vacuoles. Higher surface area/volume, nonspecific endocytosis, and membrane damage due to their rod shape can explain the higher toxicity compared to spherical shaped IONP [30], also rod-shape IONPs have been found to be endocytosed more slowly than spherical IONPs [31].

Surface area is another physical parameter that contribute with cytotoxicity of IONPs. Some researchers found that the bare Fe<sub>3</sub>O<sub>4</sub> (20–30 nm, surface area: 42 m<sup>2</sup>/g) and Fe<sub>3</sub>O<sub>4</sub> (5 µm, surface area: 6.8 m<sup>2</sup>/g) have toxicity in A549 cells in terms of cell death, mitochondrial damage, and DNA damage, but no significant difference was found between the toxicity response by Fe<sub>3</sub>O<sub>4</sub> (20–30 nm) and Fe<sub>3</sub>O<sub>4</sub> (5 µm) [32]. In contrast, higher surface area of smaller IONPs has been linked to increased toxicity of IONPs [33,34].

The oxidation state of iron (Fe<sup>2+</sup> or Fe<sup>3+</sup>) in IONPs is an additional key factor that determines the cytotoxicity of SPIONs. It has been demonstrated that Fe<sup>3+</sup> ions are much more potent in inducing DNA damage than Fe<sup>2+</sup> [35].

The bare IONPs (30 nm, 0.5 mg/mL) induced higher ROS formation compared to bare IONPs (5 nm, 0.5 mg/mL) in porcine aortic endothelial cells (PAEC), whereas dextran and PEG coated IONPs did not show any changes in ROS at similar concentrations. The same study also reported cell elongation and actin cytoskeleton disruption upon exposure to bare IONPs (30 nm, 0.5 mg/mL) [36]. Increased toxicity was observed with polyethylimine coated IONPs (50 µg/mL), whereas inclusion of PEGylation and acetylation eliminated cytotoxicity in KB cells (MTT assay). Authors claimed that the increase in toxicity can be attributed to the strong electrostatic interaction between the negatively charged cell surface and positively charged IONPs at higher doses [37].

Additionally, proteins and other nutrients in cell culture medium may be adsorbed onto IONPs and become unavailable for cellular activities, leading to the changes of cell growth and viability. Therefore, different medium recipes could influence the outcome of IONPs cytotoxicity and optimal culture medium should be determined individually according to the type of IONPs [38,39]. Also physical damage by IONPs can also cause toxicity by inducing oxidative stress in cells. It has been demonstrated that incubation with IONPs affects

the cell surface roughness which could also change the shape and alter the response by cellular cytoskeleton [40].

According to these findings from the majority of nanotoxicity studies conducted with iron oxide nanoparticles, several mechanisms were suggested to explain the cytotoxic effect of iron oxide NPs. One of the important mechanisms is that iron, not only as a catalyst but also as a reactant, may contribute to

free radical generation, which can promote the oxidation of proteins, peroxidation of membrane lipids, and modification of nucleic acids [41,42].

### Conclusion

The iron oxide nanoparticle have cytotoxic effect against cancer cell of different origins and it is safe for normal cells ,therefore it can be use alone for treatment of cancer .

## References:

1. Xie J., Huang J., Li X., Sun S., Chen X. ( 2009). Iron oxide nanoparticle platform for biomedical applications. *Curr Med Chem* , 16:1278-1294.
2. Yu M.K., Jeong Y.Y., Park J., Park S., Kim J.W., Min J.J., Kim K., Jon S. (2008). Drug-loaded superparamagnetic iron oxide nanoparticles for combined cancer imaging and therapy in vivo. *Angew Chem Int Ed Engl* , 47:5362-5365.
3. Liong M, Lu J, Kovochich M, Xia T, Ruehm SG, Nel AE, Tamanoi F, Zink JI.(2008). Multifunctional inorganic nanoparticles for imaging, targeting, and drug delivery. *ACS Nano* , 2:889-896.
4. Chouly C., Pouliquen D., Lucet I., Jeune J.J., Jallet P. (1996). Development of superparamagnetic nanoparticles for MRI: effect of particle size, charge and surface nature on biodistribution. *J Microencapsul* , 13:245-255.
5. Gupta A.K., and Gupta M. (2005). Synthesis and surface engineering of iron oxide nanoparticles for biomedical applications. *Biomaterials*, 26: 3995–4021.
6. Ito A., Shinkai M., Honda H., and Kobayashi T. (2005). Medical application of functionalized magnetic nanoparticles. *J Biosci Bioeng*, 100: 1–11.
7. Liu G., Men P., Harris P.L., Rolston R.K., Perry G., and Smith M.A. (2006). Nanoparticle iron chelators: a new therapeutic approach in Alzheimer disease and other neurologic disorders associated with trace metal imbalance. *Neurosci Lett*, 406: 189–93.
8. Silva A.C., Oliveira T.R., Mamani J.B., Malheiros S.M., Malavolta L., Pavon L.F., Sibov T.T., Amaro E. J., Tannus A., Vidoto E.L. (2011) Application of hyperthermia induced by Superparamagnetic iron oxide nanoparticles in glioma treatment. *Int J Nanomed*, 6: 591–603.
9. Johannsen M., Thiesen B., Wust P., and Jordan A. (2010). Magnetic nanoparticle hyperthermia for prostate cancer. *Int J Hyperthermia*, 26: 790–795.
10. Hilger I., and Kaiser W.A. (2012). Iron oxide-based nanostructures for MRI and magnetic hyperthermia. *Nanomedicine*, 7: 1443–1459.
11. Wei H. , and Wang E. (2013). Nanomaterials with enzyme-like characteristics (nanozymes): next-generation artificial enzymes. *Chem Soc Rev*, 42: 6060—6093.
12. Wei H., and Wang E. (2008). Fe<sub>3</sub>O<sub>4</sub> magnetic nanoparticles as peroxidase mimetic and their applications in H<sub>2</sub>O<sub>2</sub> and glucose detection. *Anal Chem*, 80(6):2250-4.
13. Brunner T.J., Wick P., Manser P., Spohn P., Grass R.N., Limbach L.K., Bruinink A., and Stark W.J. (2006). In vitro cytotoxicity of oxide nanoparticles: comparison to asbestos, silica, and the effect of particle solubility. *Environ Sci Technol*, 40 (14): 4374–81.
14. Al-Shammery, A.M. (2003). The study of Newcastle disease virus effect in treatment of transplanted tumors in mice. M.Sc. Thesis, College of Veterinary Medicine, Baghdad University.
15. Gey G.O., Coffman W.O., and Kubicek M.T. (1951).. Tissue culture studies of the proliferative capacity of cervical carcinoma and normal epithelium. *Cancer Res*, 12:264.
16. Betancur-Galvis L.B., Saez J., Granados H., Salazar A., and Ossa J. (1999). Antitumor and antiviral activity of Colombian medicinal plant extracts. *Mem Inst Oswaldo Cruz*, 94,:4:531-535.
17. Lei L., Ling J., Yun Z., and Gang L. (2013). Toxicity of Superparamagnetic iron oxide nanoparticles: Research strategies and implications for nanomedicine. *Chin Phys B*, 22 ,:12: 127503.
18. Doak S.H., Griffiths S.M., Manshian B., Singh N., Williams P.M., Brown A.P., and Jenkins G.J. (2009).Confounding experimental considerations in nanogenotoxicology. *Mutagenesis*, 24: 285–293.
19. Mahmoudi M., Simchi A., Imani M., Shokrgozar M.A., Milani A.S., Hafeli U.O., and Stroeve P. (2010).A new approach for the in vitro identification of the cytotoxicity of Superparamagnetic iron oxide nanoparticles. *Coll. Surf. B Biointerfaces*, 75: 300–309.
20. Gonzales M., Mitsumori L.M., Kushleika J.V., Rosenfeld M.E., and Krishnan K.M. (2010). Cytotoxicity of iron oxide nanoparticles made from the thermal decomposition of organometallics and aqueous phase transfer with Pluronic F127. *Contrast Media Mol. Imaging*, 5: 286–293.
21. Mahmoudi M., Hofmann H., Rothen-Rutishauser B., and Petri-Fink A. (2012). Assessing the in vitro and in vivo toxicity of Superparamagnetic iron oxide nanoparticles. *Chem Rev*, 112: 2323–2338.
22. Yang W., Lee J., Hong S., Lee J., and Han D.W. (2013). Difference between toxicities of iron oxide magnetic nanoparticles with various surface-functional groups against human normal fibroblasts and fibrosarcoma cells. *Materials*, 6: 4689–4706.
23. Daniels T.R., Delgado T., Helguera G., Penichet M.L. (2006). The transferrin receptor part II: targeted delivery of therapeutic agents into cancer cells. *Clinical Immunol*, 121: 159-76.
24. Brown D.M., Wilson M.R., MacNee W., Stone V., and Donaldson K. (2001). Size-dependent proinflammatory effects of ultrafine polystyrene particles: A role for surface area and oxidative stress in the enhanced activity of ultrafines. *Toxicolo Appl Pharmacol*, 175: 191–199.
25. Donaldson K., and Tran C.L. (2002). Inflammation caused by particles and fibers. *Inhal Toxicol*, 14(1):5-27.
26. Shen S., Liu Y., Huang P., and Wang J. (2009). In vitro cellular uptake and effects of Fe<sub>3</sub>O<sub>4</sub> magnetic nanoparticles on HeLa cells. *J Nanosci Nanotechnol*, 9,:5:2866-71.
27. Naqvi S., Samim M., Abdin M., Ahmed F.J., Maitra A., Prashant C., and Dinda A.K. (2010). Concentration-dependent toxicity of iron oxide nanoparticles mediated by increased oxidative stress. *Int J Nanomed*, 5: 983–989.
28. Dwivedi S., Siddiqui M.A., Farshori N.N., Ahamed M., Musarrat J., and Al-Khedhairi A.A. (2014). Synthesis, characterization and toxicological evaluation of iron oxide nanoparticles in human lung alveolar epithelial cells. *Coll Surf B Biointerfaces*, 122: 209–215.
29. Shukla S., Jadaun A., Arora V., Sinha R.K., Biyani N., and Jain V.K. (2015). In vitro toxicity assessment of chitosan oligosaccharide coated iron oxide nanoparticles. *Toxicol Rep*, 2: 27–39.
30. Lee J.H., Ju J.E., Kim B.I., Pak P.J., Choi E.K., Lee H.S., and Chung N. (2014). Rod-shaped iron oxide nanoparticles are more toxic than sphere-shaped nanoparticles to murine macrophage cells.

- Environ Toxicol Chem, 33: 2759–2766.
31. Mahmoudi M., Simchi A., Imani M., Milani A.S., and Stroeve P. (2008). Optimal design and characterization of Superparamagnetic iron oxide nanoparticles coated with polyvinyl alcohol for targeted delivery and imaging. *J Phys Chem B*, 112, :46:14470–14481.
  32. Karlsson H.L., Gustafsson J., Cronholm P., and Möller L. (2009). Size-dependent toxicity of metal oxide particles—A comparison between nano- and micrometer size. *Toxicol Lett*, 188: 112–118.
  33. Ying E., and Hwang H.M. (2010). In vitro evaluation of the cytotoxicity of iron oxide nanoparticles with different coatings and different sizes in A3 human T lymphocytes. *Sci Total Environ*, 408: 4475–4481.
  34. Yang L., Kuang H., Zhang W., Aguilar Z.P., Xiong Y., Lai W., Xu H., and Wei H. (2015). Size dependent biodistribution and toxicokinetics of iron oxide magnetic nanoparticles in mice. *Nanoscale*, 7: 625–636.
  35. Singh N. (2009). Nanotoxicology: Health & Environmental impacts, genotoxic potential of ultra-fine Superparamagnetic iron oxide NPs. *Nanomedicine*, 4 (4): 385-390.
  36. Yu M., Huang S., Yu K.J., and Clyne A.M. (2012). Dextran and polymer polyethylene glycol (PEG) coating reduce both 5 and 30 nm iron oxide nanoparticle cytotoxicity in 2D and 3D cell culture. *Int J Mol Sci*, 13: 5554–5570.
  37. Cai H., An X., Cui J., Li J., Wen S., Li K., Shen M., Zheng L., Zhang G., Shi X. (2013). Facile hydrothermal synthesis and surface functionalization of polyethyleneimine-coated iron oxide nanoparticles for biomedical applications. *ACS Appl Mater Interfaces*, 5: 1722–1731.
  38. Mahmoudi M., Sahraian M.A., Shokrgozar M.A., and Laurent S. (2011). Superparamagnetic iron oxide nanoparticles: promises for diagnosis and treatment of multiple sclerosis. *ACS Chem Neurosci*, 23 :118-40.
  39. Laurent S., Burtea C., Thirifays C., Häfeli U.O., and Mahmoudi M. (2012) Crucial ignored parameters on nanotoxicology: The importance of toxicity assay modifications and cell vision. *PLoS ONE*, 7;1 : 306.
  40. Hoskins C., Cuschieri A., and Wang L. (2012). The cytotoxicity of polycationic iron oxide nanoparticles: Common endpoint assays and alternative approaches for improved understanding of cellular response mechanism. *J Nanobiotechnol*, 10: 15.
  41. Valko M., Leibfritz D., Moncol J., Cronin M.T., Mazur M., and Telser J. (2007). Free radicals and antioxidants in normal physiological functions and human disease. *Int J Biochem Cell Biol*, 39;1:44-84.
  42. Wu H., Yin J.J., Wamer W.G., Zeng M., and Lo Y.M. (2014). Reactive oxygen species-related activities of nano-iron metal and nano-iron oxides. *J Food Drug Anal*, 22: 86–94.

## التأثير السمي لدقائق الحديد النانوية على بعض انواع الخلايا السرطانية في الزجاج

شذى صلاح اسعد<sup>1</sup>, د. خالد مهدي صالح<sup>2</sup>, د. ناهي يوسف ياسين<sup>3</sup>

1 جامعة بغداد/ كلية طب الكندي/ فرع التشريح

2 الجامعة المستنصرية/ كلية العلوم/ قسم علوم الحياة

3 الجامعة المستنصرية/ مركز بحوث السرطان والوراثة الطبية

### الخلاصة:

**الهدف:** قدمت التقنية النانوية امكانات كبيرة للسرطان لتشخيص السرطان والعلاج الهادف والمراقبة من بين الانواع النانوية التي تطورت سريعا هي المواد النانوية الممغنطة لإصفاها المطابقة حيويًا والوقوع مغناطيسية مع استقرارها الكيميائي وقلة سميتها يتوقع بان يكون لها مستقبل مرموق. اما عن السلامة الحيوية لهذه المواد يجب ان يتم تقديرها. هدف هذه الدراسة هو لتقييم التأثير السمي لدقائق الحديد النانوية المغناطيسية على بعض انواع خطوط الخلايا السرطانية.

**المواد وطرق العمل:** حضرت ستة تراكيز من دقائق الحديد النانوي (100, 200, 400, 600, 800, 1000 مايكروغم/مل) واختبرت على خطوط الخلايا السرطانية (AMN3, Hela, RD) مقارنة مع خط الخلايا الطبيعي REF كمجموعة سيطرة لفترة تعريض (24, 48 ساعة). تم قياس الكثافة الضوئية لتسعة مكررات للتجربة بجهاز قارئ الايلييزة بطول موجي 500 نانوميتر. استخدمت الطريقة الكمية (فحص MTT) لحساب نسبة الخلايا الحية بعد كل معالجة.

**النتائج:** اظهرت جميع خطوط الخلايا السرطانية تثبيط معنوي لكل من الكثافة الضوئية ونسبة التثبيط لنمو الخلايا السرطانية بعد 24 و48 ساعة من التعريض لجميع تراكيز الحديد النانوي, بينما اظهرت نتائج التعريض للخلايا الطبيعية ارتفاع غير معنوي  $p < 0.05$  عند مقارنتها بمجموعة السيطرة.

**الاستنتاج:** استحدثت جميع تراكيز دقائق الحديد النانوية السمية الخلوية لجميع خطوط الخلايا السرطانية مقارنة بخط الخلايا الطبيعية.